

## Cavitand-Based Nanoscale Coordination Cages

Roberta Pinalli,<sup>†</sup> Veronica Cristini,<sup>†</sup> Valerio Sottili,<sup>†,§</sup> Silvano Geremia,<sup>‡</sup> Mara Campagnolo,<sup>‡</sup> Andrea Caneschi,<sup>§</sup> and Enrico Dalcanale<sup>\*,†</sup>

Dipartimento di Chimica Organica e Industriale e UdR INSTM di Parma, Università di Parma, Parco Area delle Scienze 17/A, 43100 Parma, Italy, Dipartimento di Scienze Chimiche, Università di Trieste, Via L. Giorgieri 1, 34127 Trieste, Italy, and Dipartimento di Chimica e UdR INSTM di Firenze, Università di Firenze, Via della Lastruccia 3, 50019 Sesto Fiorentino, Italy

Received September 24, 2003; E-mail: enrico.dalcanale@unipr.it

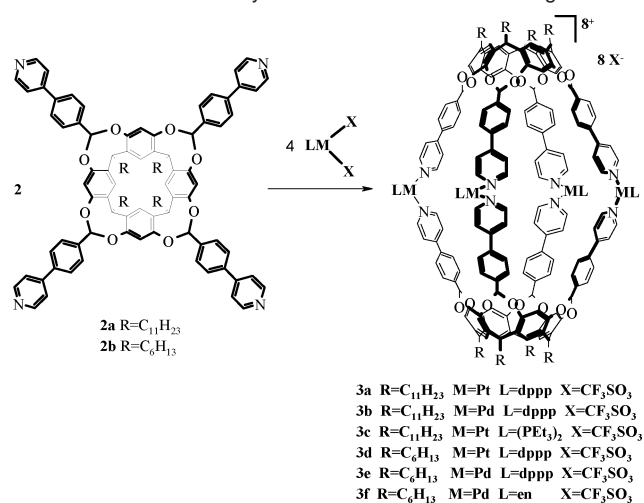
This communication describes design, self-assembly, crystal structure determination, and self-selection properties of nanoscale coordination cages formed by tetradentate deep-cavity cavitand ligands and appropriate metal precursors. Precise control over the formation and structure of nanoscale molecular architectures<sup>1</sup> is an essential prerequisite for the exploitation of these new methodologies in nanotechnology.<sup>2</sup> In fact, the successful translation of a given self-assembly procedure from solution to surfaces<sup>3</sup> requires a comprehensive understanding of all factors controlling it.<sup>4</sup> In this perspective, the formation of nanosize coordination cages on surfaces is particularly appealing for single-molecule addressing.<sup>5</sup> Cavitand-based coordination cages<sup>6</sup> are receiving increasing attention because of the versatility of cavitand platforms in terms of preorganization and synthetic modularity.

Our chosen strategy for enlarging coordination cages lies in deepening the cavitand precursor via introduction of an appropriate bridging group on the resorcinarene skeleton.<sup>7</sup> Using this approach, we have recently synthesized new picolyl-bridged cavitands, preorganized for cage self-assembly (CSA) via coordination to Pd or Pt metal precursors.<sup>8</sup> Phenyl groups were chosen as spacers to extend the cavity size,<sup>9</sup> retaining at the same time the relative orientation of the pyridine moieties and the rigidity of the cavitand framework, both pivotal for CSA.

Deep-cavity cavitands<sup>10</sup> **2a,b** were prepared by bridging the corresponding resorcinarenes **1a,b** (see Supporting Information) with 4-( $\alpha$ - $\alpha'$ -dibromo)tolylpyridine in the presence of  $K_2CO_3$  as base and DMA as solvent. The reaction gave only the oooo desired isomer, with the four phenylpyridyl arms pointing outward from the cavity, in good yield, without any experimental evidence of the presence of other possible isomers having one or more phenylpyridyl groups pointing into the cavity.

The typical procedure of cage formation is shown in Scheme 1: by simply mixing **2a** or **2b** with  $MLX_2$  complexes in 1:2 ratio at room temperature in solvents such as  $CH_2Cl_2$ ,  $C_2H_2Cl_4$ , and acetone, cages **3a–f** were obtained in quantitative yields.<sup>11</sup> All cages were fully characterized by NMR and MS analyses. The following proton resonances are diagnostic of CSA: the one belonging to the ortho pyridine protons is always shifted downfield following complexation, while the bridging protons are shifted upfield upon cage formation. <sup>31</sup>P NMR exhibited a sharp singlet, with appropriate Pt satellites for cages **3a,c** and **3d**, indicating that all the phosphorus atoms are equivalent. <sup>19</sup>F NMR recorded a sharp singlet near  $-77$  ppm for all cages, excluding permanent  $CF_3SO_3^-$  inclusion in solution. Further evidence of the cage formation was given by MALDI-TOF MS ( $[3a-X]^+$  at 7006 uma) and by ESI-FTICR MS, where the isotopically resolved signals  $[3d-3X]^{3+}$  and  $[3d-4X]^{4+}$

**Scheme 1.** Self-Assembly of Nanosize Coordination Cages **3a–f**



of cage **3d** are in agreement with the calculated isotopic distribution patterns (see Supporting Information).

Nice crystals of cage **3d** were obtained by liquid diffusion of ethanol in a  $CH_2Cl_2$  solution of the cage.<sup>12</sup> The crystal structure, determined at 100 K using synchrotron radiation, revealed the presence of cages with a pseudo  $D_{2h}$  symmetry. These cages are formed by four square-planar metal complexes in the equatorial region, connecting the two cavitand ligands (Figure 1a). The  $N(Py)-Pt-N(Py)$  bond angles (from  $83.4^\circ$  to  $84.9^\circ$ ) and those of  $P(dppp)-Pt-P(dppp)$  (from  $90.8^\circ$  to  $92.6^\circ$ ) indicate a small distortion in the coordination sphere at the Pt metal centers. All triflates are positioned outside the cavity, near the four Pt centers: four triflates positioned on the smaller lateral portals strongly interact with the metals by the oxygen (distance  $O-Pt \approx 3 \text{ \AA}$ ), while the other four, which are located on the larger lateral portals, on the same side of the phenyl groups of the dppp, are away from the metal center (distance  $O-Pt \approx 4 \text{ \AA}$ ) (Figure 1b). In the cavity near the resorcinarene bowl of both cavitands, two molecules of ethanol have been found (Figure 1a), and an unknown electronic density, probably some disordered solvent molecules, has been detected in the equatorial part of the cavity (not reported in Figure 1). From the crystal structure the dimensions of the lateral portals and those of the internal cavity have been determined, respectively, as  $17.1 \times 17.6 \text{ \AA}$  and  $22.9 \times 22.3 \text{ \AA}$ .

Computer simulations using GRASP<sup>13</sup> estimated the internal volume of the cavity in  $1800 \text{ \AA}^3$ , more than twice that of the picolyl-bridged analogue cage **5** ( $840 \text{ \AA}^3$ ).<sup>8</sup>

Reversibility of CSA in the presence of a competitive ligand can be turned on/off by changing the metal. By adding 8 equiv of  $NEt_3$  to a solution of Pd-cage **3b** and heating to  $50^\circ C$ , the free

<sup>†</sup> Università di Parma.  
<sup>‡</sup> Università di Trieste.  
<sup>§</sup> Università di Firenze.

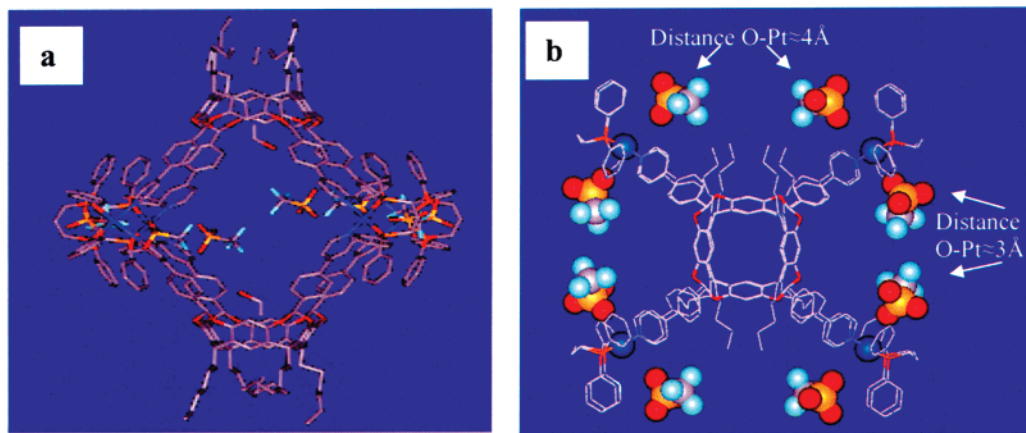


**Figure 1.** Crystal structure of **3d**. (a) Side view. Two ethanol molecules are visible in the cavity. (b) Top view. The eight triflates are placed outside the cavity, near the metal centers.

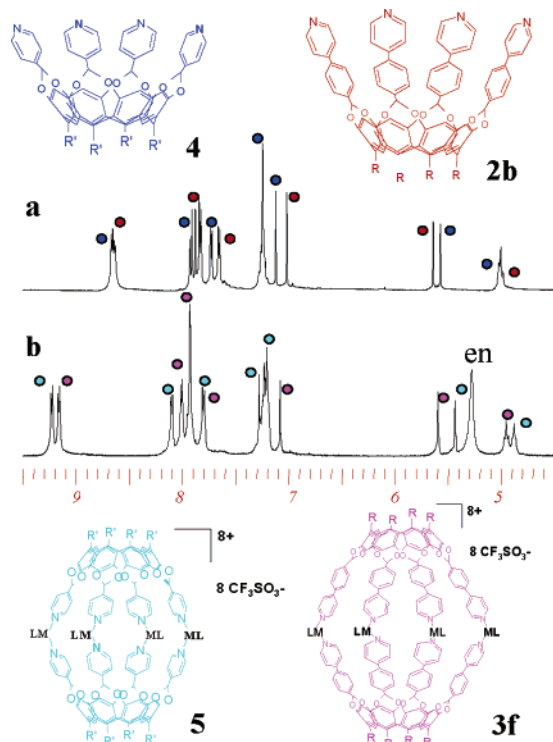


**Figure 2.** Self-recognition of cavitands **2b** and **4** ( $R' = \text{CH}_2\text{CH}_2\text{Ph}$ ) monitored by  $^1\text{H}$  NMR. (a) Spectral window of cavitands **2b** and **4** in acetone- $d_6$ . (b) Cages **3f** and **5** as single products after addition of 2 equiv of  $\text{Pd}(\text{en})(\text{CF}_3\text{SO}_3)_2$ .

cavitand was obtained, while the corresponding Pt-cage **3a** was stable under the same conditions.

A competition experiment has been performed to verify the self-selection properties of CSA. For this experiment, we chose two different cavitands: picolyl-bridged cavitand **4**<sup>8</sup> and tolylpyridyl-bridged cavitand **2b**. After addition of a stoichiometric amount of the metal precursor to an equimolar mixture of cavitand **2b** and its picolyl-bridged analogue **4**, only the signals belonging to homocages **3f** and **5** were detected (Figure 2). The mismatch between the biting angles of the two cavitand ligands leads to complete self-recognition during the CSA process.

In summary, we reported design, self-assembly, and structural characterization of nanoscale cavitand-based coordination cages.

The precise control of the CSA process over formation, dissolution, and self-selection of these coordination cages opens new possibilities for the generation and single-molecule addressing of such three-dimensional architectures directly on surfaces.<sup>14</sup>

**Acknowledgment.** This work was supported by MURST (FIRB Projects RBNE01YLKN and RBAU01HAAA). We warmly thank Prof. P. Vainiotalo for high resolution ESI-FTICR MS spectra. This paper is dedicated to the memory of Roberto Santi.

**Supporting Information Available:** Experimental procedures and spectral data for all new compounds, including ESI-FTICR MS spectra of **3d**, ORTEP view (PDF), and crystallographic data (CIF). This material is available free of charge via the Internet at <http://pubs.acs.org>.

## References

- (1) (a) Brückner, C.; Powers, R. E.; Raymond, K. N. *Angew. Chem., Int. Ed.* **1998**, *37*, 1837–1839. (b) Takeda, N.; Umemoto, K.; Yamaguchi, K.; Fujita, M. *Nature* **1999**, *398*, 794–796. (c) Olenyuk, B.; Whiteford, J. A.; Fechtenkötter, A.; Stang, P. J. *Nature* **1999**, *398*, 796–799.
- (2) (a) Special section on supramolecular chemistry and self-assembly: *Science* **2002**, *295*, 2395–2421. (b) Holliday, B. J.; Mirkin, C. A. *Angew. Chem., Int. Ed.* **2001**, *40*, 2022–2043.
- (3) Levi, S. A.; Guatteri, P.; van Veggel, F. C. J. M.; Vancso, G. J.; Dalcanele, E.; Reinhoudt, D. N. *Angew. Chem., Int. Ed.* **2001**, *40*, 1892–1896.
- (4) Fochi, F.; Jacopozi, P.; Wegelius, E.; Rissanen, K.; Cozzini, P.; Marastoni, E.; Fiscaro, E.; Manini, P.; Fokkens, R.; Dalcanele, E. *J. Am. Chem. Soc.* **2001**, *123*, 7539–7552.
- (5) Friggeri, A.; van Manen, H.-J.; Auletta, T.; Li, X.-M.; Zapotoczny, S.; Schönherr, H.; Vancso, G. J.; Huskens, J.; van Veggel, F. C. J. M.; Reinhoudt, D. N. *J. Am. Chem. Soc.* **2001**, *123*, 6388–6395.
- (6) (a) Jacopozi, P.; Dalcanele, E. *Angew. Chem., Int. Ed.* **1997**, *36*, 613–615. (b) Fox, O. D.; Dalley, N. K.; Harrison, R. G. *J. Am. Chem. Soc.* **1998**, *120*, 7111–7112. (c) Fox, O. D.; Drew, M. G. B.; Beer, P. D. *Angew. Chem., Int. Ed.* **2000**, *39*, 136–140. (d) Park, S. J.; Hong, J.-I. *Chem. Commun.* **2001**, 1554–1555.
- (7) Green, J. O.; Baird, J.-H.; Gibb, B. C. *Org. Lett.* **2000**, *2*, 3845–3848.
- (8) Pirondini, L.; Bertolini, F.; Cantadori, B.; Ugozzoli, F.; Massera, C.; Dalcanele, E. *Proc. Natl. Acad. Sci. U.S.A.* **2002**, *99*, 4911–4915.
- (9) Cuminetti, N.; Ebbing, M. H. K.; Prados, P.; de Mendoza, J.; Dalcanele, E. *Tetrahedron Lett.* **2001**, *42*, 527–530.
- (10) For a review on deep-cavity cavitands, see: Rudkevich, D. M.; Rebek, J., Jr. *Eur. J. Org. Chem.* **1999**, 1991–2005.
- (11) CSA is fully effective in a wide concentration (0.8–8 mM) and temperature range (253–373 K).
- (12) Crystal data of **3d**:  $(\text{C}_{316}\text{H}_{504}\text{N}_{80}\text{O}_{40}\text{Pt}_4\text{P}_8\text{S}_8\text{F}_{24})(\text{C}_{10}\text{H}_{22}\text{O}_6)(\text{C}_6\text{H}_{14}\text{O}_4) \cdot 1.5(\text{C}_4\text{H}_{10}\text{O}_3) \cdot 18(\text{C}_2\text{H}_6\text{O})(\text{C}_2\text{H}_6\text{O}_2)$ ; fw = 8095.26; monoclinic; space group  $P2_1/c$ ;  $a = 25.2946(13)$  Å,  $b = 38.8640(11)$  Å,  $c = 50.4327(19)$  Å,  $\beta = 93.234(2)^\circ$ ;  $V = 49499(3)$  Å<sup>3</sup>;  $d_{\text{calcd}} = 1.086$  g cm<sup>-3</sup>;  $Z = 4$ . The final refined  $R$  value was 0.110. Full details are described in the Supporting Information.
- (13) Mecozzi, S.; Rebek, J., Jr. *Chem.-Eur. J.* **1998**, *6*, 1016–1022.
- (14) Menozzi, E.; Pinalli, R.; Speets, E. A.; Ravoo, B. J.; Dalcanele, E.; Reinhoudt, D. N. *Chem.-Eur. J.* **2004**, *10*, 2199–2206.

JA038694+